Arab J Geosci (2017) 10: 400
DOI 10.1007/s12517-017-3146-2

ORIGINAL PAPER

Heterogeneity analysis of reservoir porosity and permeability in the Late Ordovician glacio-fluvial Sarah Formation paleovalleys, central Saudi Arabia

Islam El-Deek[1] · **Osman Abdullatif**[1,2] · **Gabor Korvin**[1,2]

Received: 13 February 2017 / Accepted: 4 August 2017 / Published online: 14 September 2017

Abstract The Late Ordovician glacio-fluvial Sarah Formation is an important tight gas reservoir target in Saudi Arabia. This study uses statistical methods to characterize the petrophysical heterogeneity of the paleovalleys of the Sarah Formation that crop out in central Saudi Arabia. Four paleovalleys were studied: Bukayriyah, Hanadir, Sarah, and Khanasir Sarah. Several lithofacies were identified in each that vary in texture, porosity, permeability, and facies abundance that reflect periods of ice advance and retreat. The heterogeneity analysis is based on three statistical measures, namely, the coefficient of variation, the Dykstra-Parsons coefficient, and the Lorenz coefficient. The coefficient of variation values is in the 0.62–1.94 range, indicating an extremely heterogeneous distribution. The Dykstra-Parsons coefficient values are in the 0.56–0.88 range, suggesting very high to extremely high heterogeneity in the reservoirs. The Lorenz coefficient correlates well with the Dykstra-Parsons coefficient for paleovalleys of the Sarah Formation. The heterogeneity parameters studied here indicate that the outcrops of Sarah Formation paleovalleys represent heterogeneous to very heterogeneous reservoirs, which may be attributed to complex depositional and diagenetic variations that have affected the porosity and permeability distribution.

✉ Islam El-Deek
ideek@kfupm.edu.sa

[1] Geosciences Department, King Fahd University of Petroleum and Minerals, Dhahran, Saudi Arabia

[2] Reservoir Characterization Research Group, King Fahd University of Petroleum and Minerals, Dhahran, Saudi Arabia

Keywords Sarah Formation · Reservoir heterogeneity · Petrophysical properties · Statistical measures · Dykstra-Parsons · Lorenz coefficient

Introduction

Petrophysical properties such as porosity and permeability are important indicators of oil or gas reservoir quality, and studying them enhances understanding of the reservoir and potential to predict subsurface characteristics (Morton-Thompson and Woods 1993; Sahin and Saner 2001; Selley 1998; Wilson 1994). Various factors control the properties and distribution of porosity and permeability within clastic reservoir rocks. These include texture, fabric, depositional environment, sorting, packing, amount of matrix, degree of cementation, and other post-depositional diagenetic changes. It is this relatively large number of factors, each of which can vary considerably, that result in the complexity of porosity and permeability evident in sandstone reservoirs (Abdulkadir et al. 2010; Ali et al. 2010; Boggs 2006; Fitch et al. 2015; Gier 2000; Kassab et al. 2015; Ketzer et al. 2002; Sun et al. 2007; Surdam et al. 1989).

This study investigates the Late Ordovician Sarah Formation that crops out in the Qassim region in central Saudi Arabia (Fig. 1). The Sarah Formation in this region is exposed in several glacial paleovalleys in central and northern Saudi Arabia. A stratigraphically equivalent formation to the Sarah Formation is the Late Ordovician Sanamah Formation, which is exposed in the Wajid basin in southwestern Saudi Arabia. The Sarah Formation and its equivalents occupy several sub-basinal areas and represent important subsurface tight gas exploration targets in northern and central Saudi Arabia, and in the Rub' al Khali basin to the southeast (Abdullatif 2011; Evans et al. 1991; Konert et al. 2001). Subsurface

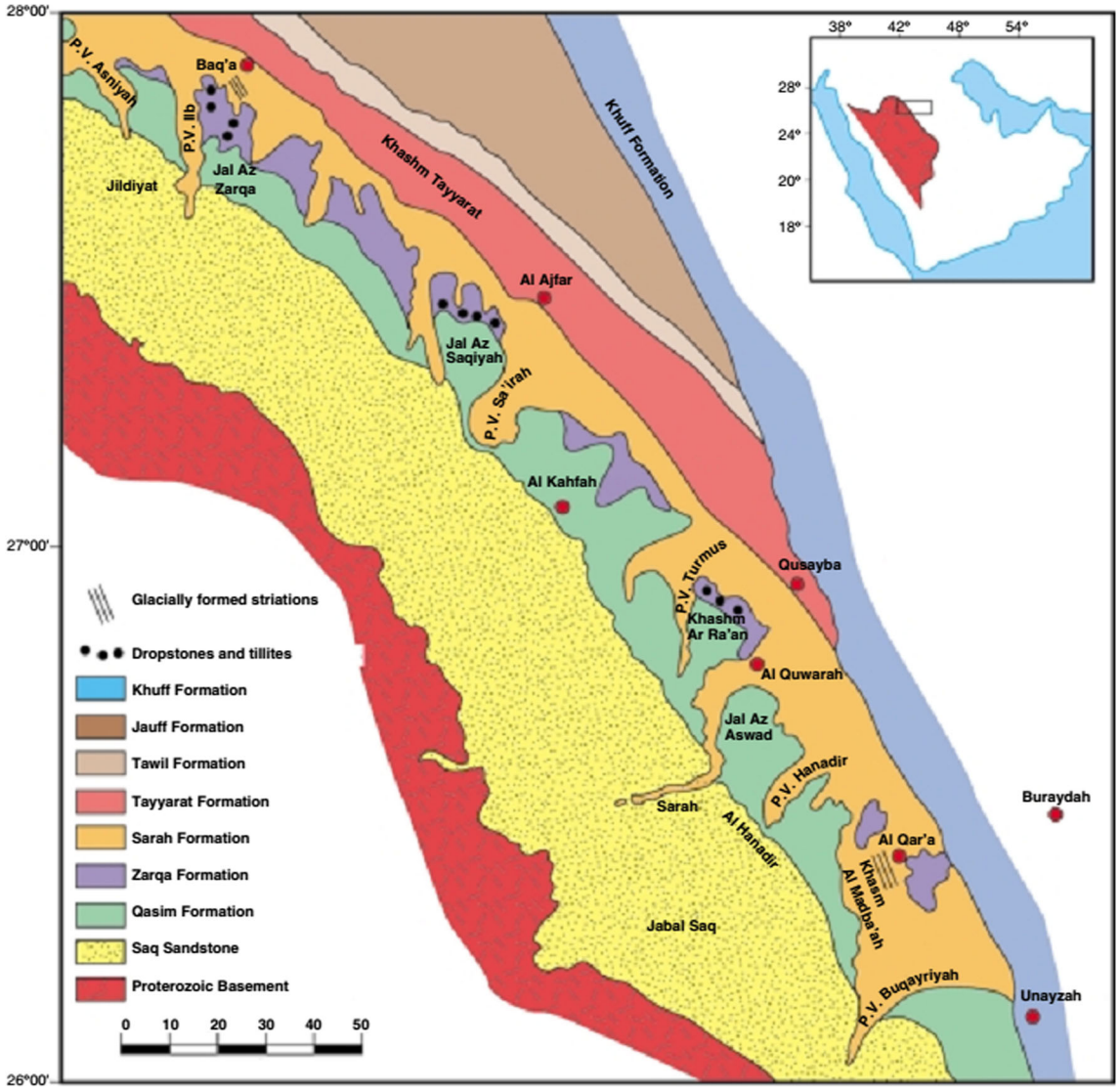

Fig. 1 Geological map showing the Late Ordovician glacio-fluvial paleovalleys (denoted by P.V.) of the Sarah Formation, central Saudi Arabia. Note the positions of the Bukayriyah, Hanadir, Sarah, and Khanasir Sarah paleovalleys (Senalp and Al-Laboun 2000)

exploration of the Paleozoic succession has revealed a complexity of facies, paleoenvironments, and paleogeography (Al-Mahmoud and Al-Ghamdi 2010; Briner et al. 2010; Khalil 2012). However, very little data are available concerning quantitative assessment of the porosity and permeability properties in the Sarah Formation in these paleovalleys. This study describes and evaluates sedimentological heterogeneity and its impact on porosity and permeability in the Sarah Formation that is exposed in the glacial paleovalleys of the Qassim region of central Saudi Arabia.

Geological background

Late Ordovician glaciation resulted in the formation of unconformities and overlying glacial, glacio-marine, and glacio-fluvial deposits laid down as influxes into deeply incised paleovalleys (McClure 1978; Senalp and Al-Laboun 2000). The Sarah Formation is characterized by low porosity and very low permeability, and considered an important tight gas reservoir target in northwestern Saudi Arabia and the Rub' al Khali basin (McGillivray and Husseini 1992).

Vaslet (1987, 1989, 1990) carried out mapping projects in the Sarah paleovalleys, while Senalp and Al-Laboun (2000) studied the sedimentological significance of the Late Ordovician Zarqa and Sarah Formations in the Qassim and Hail regions of Saudi Arabia. Paleovalleys of the Sarah Formation were thoroughly investigated by Clark-Lowes (2005) with extensive image-based and sedimentological work. In addition, Moscariello et al. (2009) studied the sedimentology and paleogeography of the Sarah Formation based on well data and outcrop observations. Several recent studies

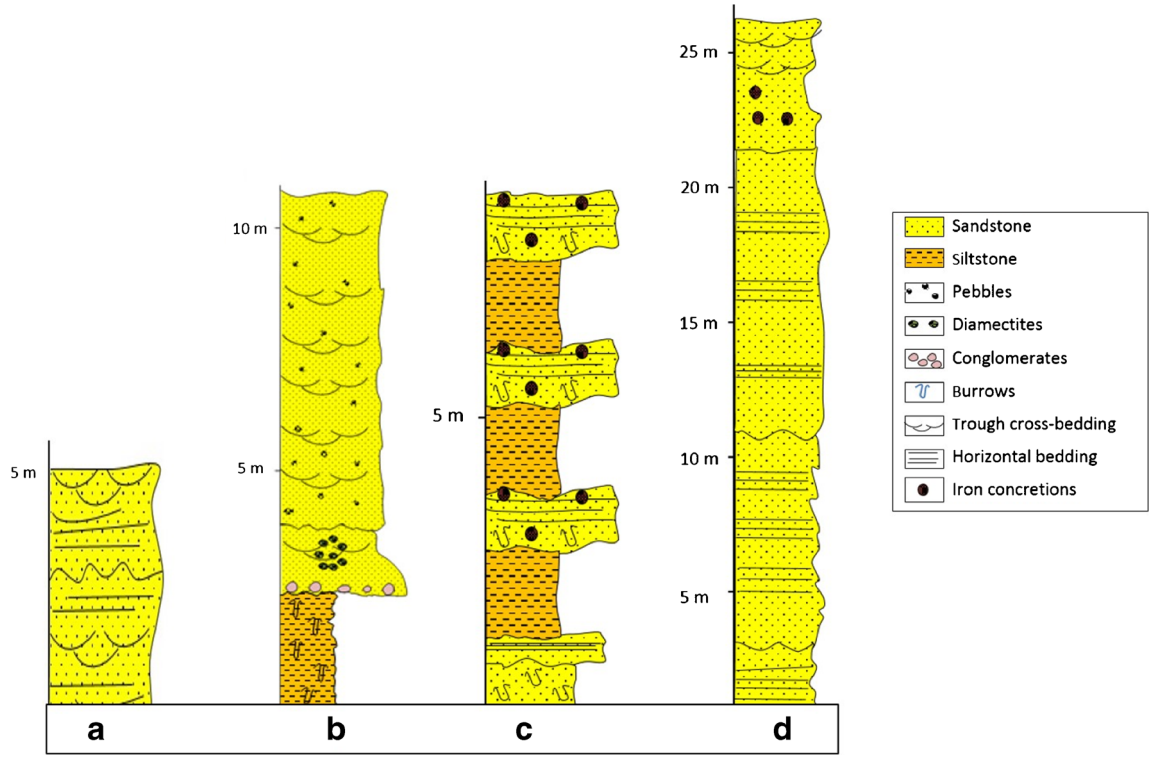

Fig. 2 Representative lithofacies sections of the glacio-fluvial paleovalleys of the Sarah Formation. **a** Interbedded trough cross-bedded sandstone. **b** Laminated siltstone overlain by pebbly cross-bedded sandstone. **c** Stacked horizontally bedded sandstone and laminated siltstone. **d** Horizontally bedded sandstone interbedded with minor trough cross-bedded sandstone and diagenetic hematite (H) and limonite (L) concretions (millimeters in size)

Table 1 Facies types recognized in the Sarah Formation paleovalleys; facies codes modified after Miall (1996)

Facies code	Facies	Sedimentary structures	Interpretation
Sh	Sand, very fine to very coarse, may be pebbly	Horizontal lamination parting or streaming lineation	Plane-bed flow (critical flow)
St	Sand, fine to very coarse, may be pebbly	Solitary or grouped trough cross-beds	Sinuous-crested and linguoid (3-D) dunes
Sl	Sand, fine to coarse, may be pebbly	Low-angle (< 15°) cross-beds	Scour fills, humpback or washed-out dunes, antidunes
Sm	Sand, fine to coarse	Massive or faint lamination	Sediment-gravity flow deposits
Ss	Sand, fine, may be pebbly	Broad, shallow scours	Scour fills
Sp	Sand, medium to coarse, pebbly	Solitary planar cross-beds	Transverse and linguoid bedforms (2D dunes)
Fl	Silt	Fine lamination, very small ripples	Overbank, abandoned channel, or waning flood deposits
Fr	Silt	Massive, roots, bioturbation	Root bed, incipient soil

of the Sarah Formation have dealt with the facies, paleoenvironments, and sandstone composition in the Wajid basin of southwestern Saudi Arabia (Abdullatif 2011, Abdullatif et al. 2013), while Al-Zayer et al. (2013) carried out well testing analysis on Sarah Formation reservoirs in the subsurface. Other works have studied reservoir heterogeneity and diagenesis (El-Deek and Abdullatif 2013; El-Deek et al. 2013; El-Deek et al. 2014a), integration of sedimentology, petrophysics, heterogeneity and statistics (El-Deek et al. 2014b), and sedimentological and petrophysical heterogeneity of a glacial paleovalley of the Sarah Formation in the Hail region of central Saudi Arabia (Razzaq et al. 2014).

Heterogeneity

Heterogeneity in a sandstone reservoir depends on various controlling factors, such as geometry, reservoir structural parameters, facies distribution, sedimentary structures, lamination, and bedding, as well as the effects of diagenesis on both porosity and permeability (Ahmed 2010; Higley et al. 1997; Milliken 2001; Morad et al. 2010). The diagenetic factors, such as compaction, cementation, leaching, and dissolution, may affect the petrophysical parameters either by preservation, destruction, or enhancement. Thus, heterogeneity occurs

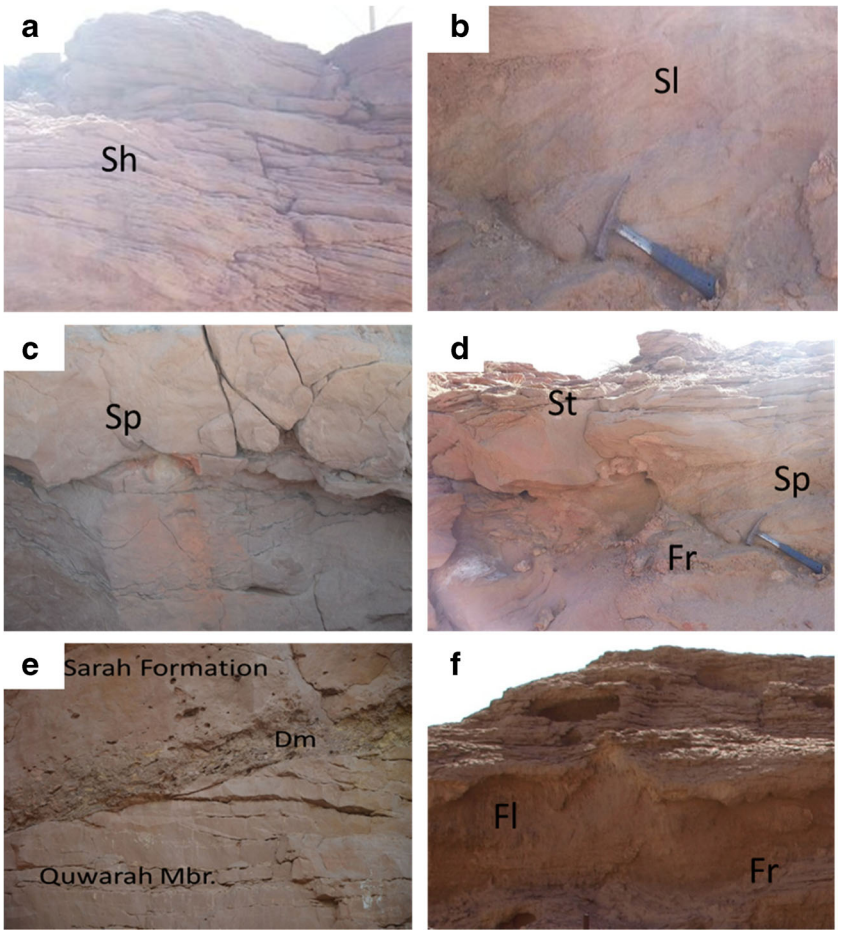

Fig. 3 Photographs showing the lithofacies sections of the glaciofluvial paleovalleys of the Sarah Formation. **a** Horizontally stratified sandstone (Sh). **b** Low-angle cross-stratified sandstone (Sl). **c** Planar cross-stratified sandstone (Sp). **d** Trough cross-stratified sandstone (St), planar cross-stratified sandstone (Sp), and massive rootlet siltstone (Fr). **e** Glacial diamictite (Dm). **f** Finely laminated (Fl) and rippled (Fr) siltstone facies

at different scales: (1) a megascopic scale (basin-scale paleogeography), (2) a macroscopic scale (formation-scale depositional environments and relationships with other Paleozoic formations), (3) a mesoscopic scale (the lithofacies variability), and (4) a microscopic scale (the factors controlling the variation of petrophysical properties, e.g., textural, compositional, depositional, and diagenetic factors) (Adams et al. 2011; Jennings Jr and Ward 2000; Pranter et al. 2006; Sahoo et al. 2016; Tiab and Donaldson 2004).

Heterogeneity can be measured as a geostatistical characteristic that provides numerical values for studying the distribution thereof, and these values can be used for comparing heterogeneity with other distributions or in other

Table 2 The lithofacies within the Sarah Formation paleovalleys with their codes and percentage abundances

Lithofacies code	Thickness (cm)	Abundance (%)
Horizontally stratified sandstone (Sh)	6420	61.38
Trough cross-stratified sandstone (St)	1760	16.83
Massive sandstone (Sm)	1430	13.67
Laminated siltstone (Fl)	780	7.46
Glacial diamectite (Dm)	50	0.48
Horizontal imbricated gravels (Gh)	20	0.18
7Total thickness	10,460	

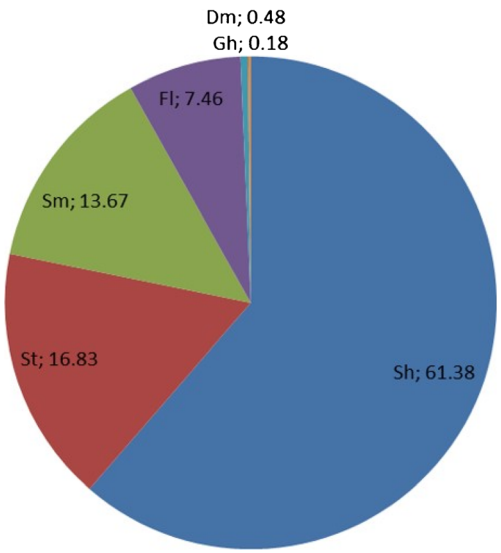

Fig. 4 Pie chart showing the lithofacies abundances in the Sarah Formation outcrops which indicates the predominance of stratified sandstone (Sh), cross-stratified sandstone (St), and massive sandstone (Sm). Fl finely laminated siltstone, Dm glacial diamictite, Gh horizontally imbricated gravels

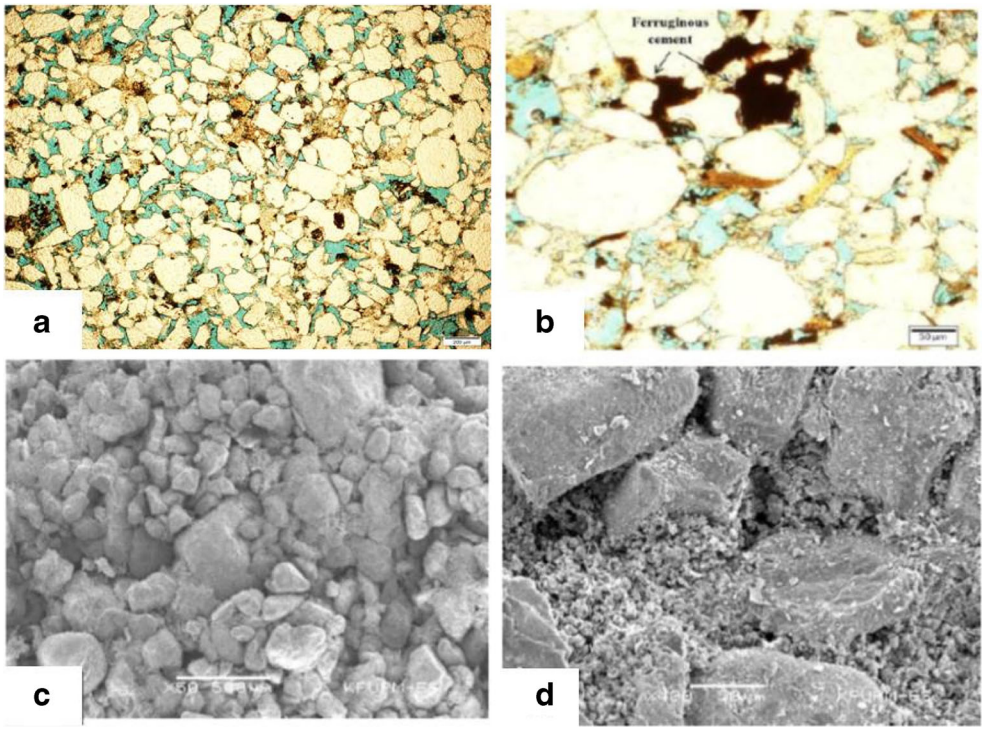

Fig. 5 Microphotographs showing **a** thin section image (in plane polarized light) of moderately sorted, sub-angular to sub-rounded clasts in quartz arenite (φ = 22.8%, K = 9.45 mD); **b** thin section image (in plane polarized light) of grain dissolution and presence of ferruginous cement between the quartz grains (φ = 30.21%, K = 26.81 mD); **c** SEM image of quartz arenite with primarily rounded to sub-rounded quartz grains (φ = 32.24%, K = 1056.5 mD); and **d** SEM image of quartz arenite with kaolinite cement blocking pore spaces between quartz grains (φ = 27.69%, and K = 1.87 mD)

reservoirs (Jensen 2000; Lake and Jensen 1991). The heterogeneity of the sandstone reservoir of the Sarah Formation is discussed in this study on the basis of the three most common statistical measures: coefficient of variation, Dykstra-Parsons coefficient, and Lorenz coefficient.

Methods and data set

This study is based on field and laboratory investigations. The field investigation involves lithofacies descriptions and analysis of the four paleovalleys (Bukayriyah, Hanadir, Sarah, and Kanasir Sarah) of the Sarah Formation in the Qassim region. The outcropping sections were studied in the field, and rock samples were collected.

The laboratory investigations included thin section petrography, X-ray powder diffraction (XRD), and scanning electron microscopy (SEM) analysis. Porosity and permeability measurements were also performed on the sandstone lithofacies.

Lithofacies description and analysis

Lithofacies descriptions, analysis, and classification were carried out on vertical and lateral outcrop sections in each of the paleovalleys. The lithofacies identified in these sections include trough cross-stratified sandstone, horizontally and low-angle stratified sandstone, planar cross-stratified sandstone, massive sandstone, shallow scour sandstone, finely laminated rippled siltstone, massive siltstone, and stratified glacial diamictite (Fig. 2). With the exception of the stratified glacial diamictite, all facies represent periods of ice retreat that is reflected in the glacial braided plain outwash facies within channels and overbank sub-environments. The glacial diamictite represents periods of ice advance. The lithofacies characteristics within the Sarah Formation paleochannel are summarized in Table 1.

Grain sizes vary from silt to very fine sand and ultimately very coarse sand. Pebbles also occur locally. The measured porosity is in the 17–56.7% range, with an average value of 28%. Permeability values are in the 0.1 mD to 2.27 Darcy range, with an average value of 0.25 Darcy. Porosity and permeability values for the Sarah Formation show variation at the outcrop scale (Fig. 3). Lithofacies within the Sarah Formation and their abundances are shown in Table 2 and Fig. 4. The sandstones are classified as quartz arenites, with angular to sub-rounded clasts that are poorly to moderately sorted, or well sorted (Fig. 5).

Statistical measures of heterogeneity

Coefficient of variation

The coefficient of variation (CV) is used as a measure of heterogeneity and is calculated by dividing the standard

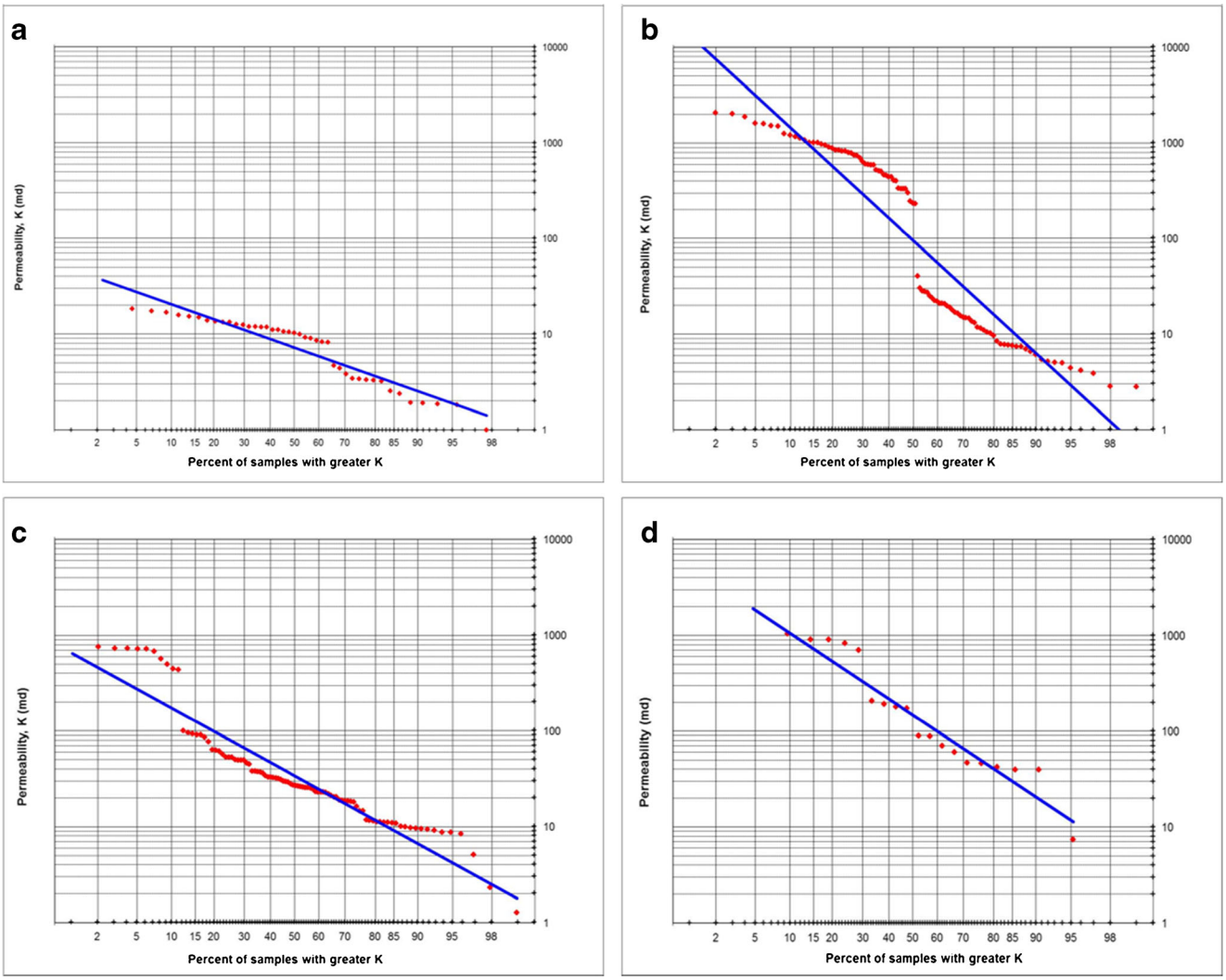

Fig. 6 Dykstra-Parsons plot of permeability for Bukayriyah paleovalley ($k_{0.50}$ = 7.2, $k_{84.1}$ = 3.2) (**a**); Hanadir paleovalley ($k_{0.50}$ = 95, $k_{84.1}$ = 11) (**b**); Sarah paleovalley ($k_{0.50}$ = 34.05, $k_{84.1}$ = 9.56) (**c**), and Khanasir Sarah paleovalley ($k_{0.50}$ = 147.47, $k_{84.1}$ = 31.72) (**d**)

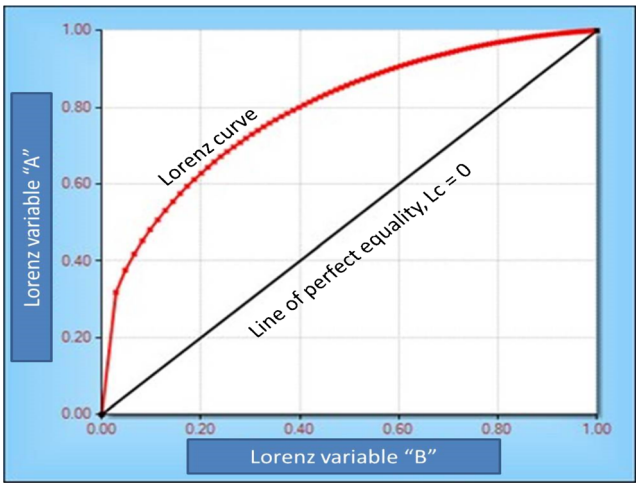

Fig. 7 Schematic illustration of a Lorenz plot showing the Lorenz curve, and line of perfect equality where Lc = 0 (after Fitch et al. 2013)

deviation of a set of samples by the mean of those samples, provided that the mean does not equal zero.

$$\mathrm{CV} = \frac{\sigma}{\mu} \tag{1}$$

where, CV is the coefficient of variation, σ is the standard deviation, and μ is the mean.

The CV of permeability values is < 0.5 in a homogenous medium, between 0.5 and 1.0 in a heterogeneous medium, and > 1.0 in a medium that is very heterogeneous (Lake and Jensen 1991).

Permeability distributions in the Bukayriyah, Hanadir, Sarah, and Khanasir Sarah paleovalleys have CV values of 0.62, 1.24, 1.94, and 1.17, respectively. These values indicate heterogeneous to very heterogeneous permeability distributions.

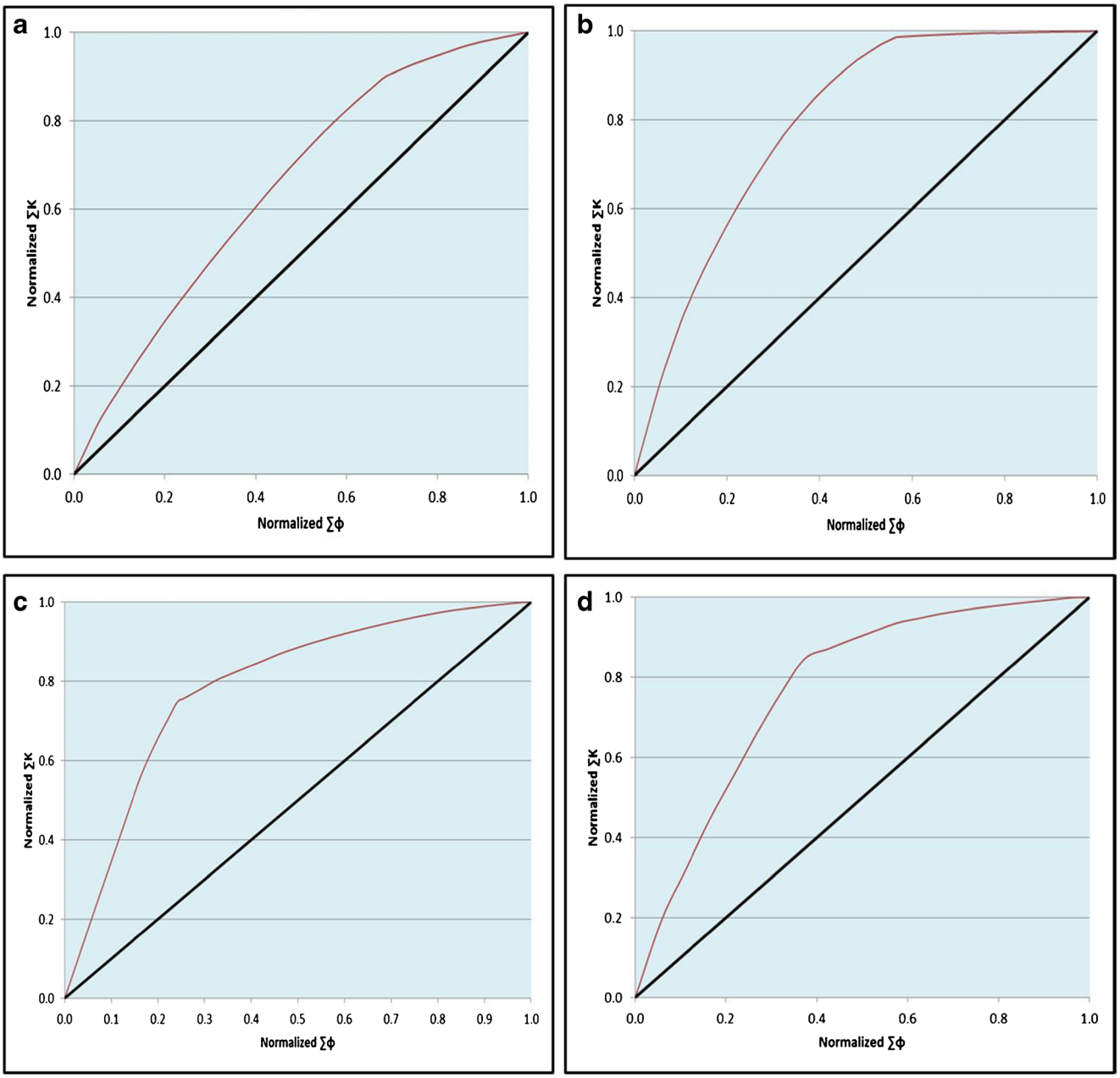

Fig. 8 Lorenz plot showing normalized porosity values (∑Ø) plotted as a function of the normalized cumulative permeability values (∑K) for **a** Bukayriyah, **b** Hanadir, **c** Sarah, and **d** Khanasir Sarah paleovalleys

Dykstra-Parsons coefficient

The Dykstra-Parsons coefficient (Dykstra and Parsons 1950) is also known as the "coefficient of permeability variation" or the "Reservoir Heterogeneity Index". It is the most common measure of heterogeneity. Tiab and Donaldson (2004) described it as an excellent tool for characterizing the heterogeneity of a reservoir. It is based mainly on permeability variations, and is calculated as follows:

$$V_{DP} = \frac{k_{0.50} - k_{84.1}}{k_{0.50}} \quad (2)$$

where, $k_{0.50}$ is the median permeability and $k_{84.1}$ is the permeability value at one standard deviation above $k_{0.50}$ on a log-permeability probability plot. The value of V_{DP} is equal to zero for an ideally homogeneous reservoir, 0–0.25 for a slightly heterogeneous reservoir, 0.25–0.5 for a heterogeneous reservoir, 0.5–0.75 for a very heterogeneous reservoir, 0.75–1 in an extremely heterogeneous reservoir, and > 1 for a perfectly heterogeneous reservoir (Tiab and Donaldson 2004).

The Dykstra-Parsons coefficient has been calculated from a set of permeability values from the Sarah Formation paleovalleys. The permeability measurements from each outcrop are sorted in descending order, followed by computation

Table 3 Heterogeneity parameters for the Sarah Formation paleovalleys

Paleovalley	Bukayriyah		Hanadir		Sarah		Khanasir Sarah	
Lithofacies	Sh, St, Sm, Dm		Sh, St, Sm		Sh, St, Gh		Sh, St, Fl	
No. of core plugs	44	44	100	100	97	97	21	21
Petrophysical properties	Ø (%)	*K* (mD)	Ø (%)	*K* (mD)	Ø (%)	*K* (mD)	Ø (%)	*K* (mD)
Mean	26.81	9.66	28.06	459.89	27.77	106.88	26.36	398.45
Median	26.68	10.41	29.01	237.70	23.36	26.99	27.87	172.76
Standard deviation	2.24	6.00	3.36	570.78	10.77	207.81	3.05	465.23
Coefficient of variation	0.08	0.62	0.12	1.24	0.39	1.94	0.12	1.17
Dykstra-Parsons coefficient	0.56		0.88		0.72		0.78	
Lorenz coefficient	0.30		0.59		0.58		0.54	
Heterogeneity	Heterogeneous to very heterogeneous reservoirs							

of the percent of permeability values greater than each permeability value in the distribution (Tables 4, 5, 6, and 7). Finally, the results are plotted on a log-probability curve (Fig. 6). The Dykstra-Parsons coefficient of permeability variation is then calculated for each of the four paleovalleys, as described below:

For Bukayriyah paleovalley:

$$k_{0.50} = 7.2, k_{84.1} = 3.2; V_{DP} = (k_{50} - k_{84.1}) \Big/ k_{50} = (7.2 - 3.2) \Big/ 7.2 = 0.56 \quad (3)$$

For Hanadir paleovalley:

$$k_{0.50} = 95, \quad k_{84.1} = 11; V_{DP} = (k_{50} - k_{84.1}) \Big/ k_{50} = (95 - 11) \Big/ 95 = 0.88 \quad (4)$$

For Sarah paleovalley:

$$k_{0.50} = 34.05, \quad k_{84.1} = 9.56; V_{DP} = (k_{50} - k_{84.1}) \Big/ k_{50} = (34.05 - 9.56) \Big/ 7.2 = 0.72 \quad (5)$$

For Khanasir Sarah paleovalley:

$$k_{0.50} = 147.47, \quad k_{84.1} = 31.72; V_{DP} = (k_{50} - k_{84.1}) \Big/ k_{50} = (147.47 - 31.72) \Big/ 7.2 = 0.78 \quad (6)$$

The range of Dykstra-Parsons coefficients indicates that the Sarah Formation reservoir is very heterogeneous to extremely heterogeneous (0.56–0.88). The Bukayriyah and Sarah paleovalleys represent very heterogeneous reservoirs, whereas the Hanadir and Khanasir Sarah paleovalleys are extremely heterogeneous.

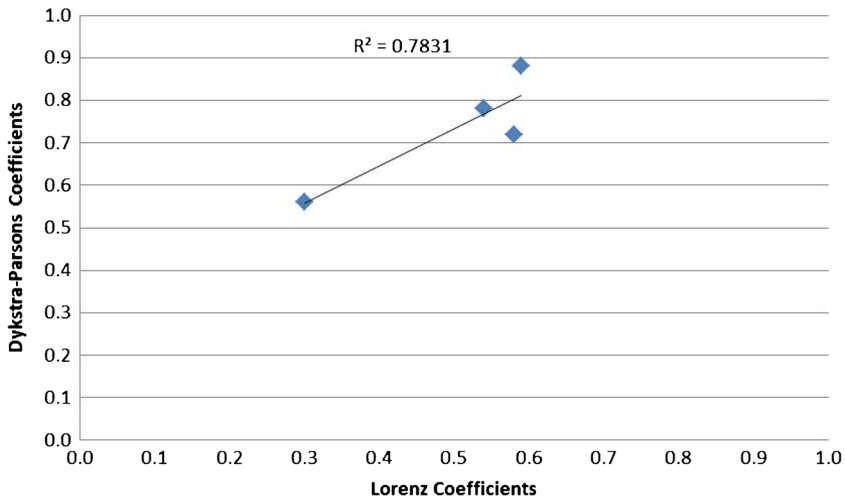

Fig. 9 Graphical illustration of the correlation between the Lorenz and Dykstra-Parsons coefficients for the Sarah Formation paleovalleys (R^2 = 0.7831)

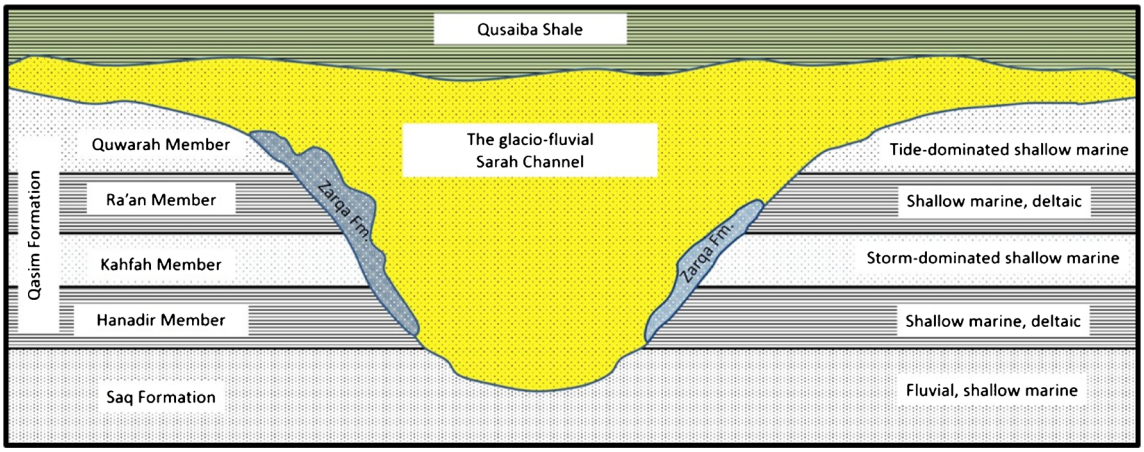

Fig. 10 Schematic model illustrating the heterogeneity of the Sarah Formation in terms of vertical and lateral facies variability and relationships with other Paleozoic formations

Lorenz coefficient

Lorenz (1905) developed the Lorenz coefficient (Lc) as a measure of the concentration of wealth. It was later introduced to geostatistics as an important parameter for characterizing the heterogeneity of porosity and permeability within a reservoir (Schmalz and Rahme 1950).

Generally, the Lc is obtained by plotting cumulative flow capacity (F_m) against cumulative thickness (H_m). The values of F_m and H_m are calculated from the following equations (Ahmed 2010; Lake and Jensen 1991; Peters 2012; Schmalz and Rahme 1950; Tiab and Donaldson 2004):

$$F_m = \frac{\sum_{i=1}^{i=m} k_i h_i}{\sum_{i=1}^{i=n} k_i h_i} \quad (7)$$

$$H_m = \frac{\sum_{i=1}^{i=m} h_i}{\sum_{i=1}^{i=n} h_i} \quad (8)$$

However, Fitch et al. (2013) developed an alternate version of the Lc in the event that there are pairs of variables that are all positive, and every pair is measured at the same location and the thickness (h) is not known. The alternate version takes the cumulative sums of the first variable "A", sorts them in descending order, and then these values are plotted against the cumulative sums of the other variable "B" (Fig. 7). Thus, the Lc can be calculated directly from porosity and permeability.

The Lc, which is twice the area between the Lorenz curve and the diagonal line in Fig. 7, ranges from zero in a homogeneous reservoir to one in a heterogeneous reservoir.

The total area below the Lorenz curve is calculated as follows:

$$\textit{Area below Lorenz curve} = \sum_{i=1}^{i=n} \left(\varnothing_{\text{cum, i+1}} - \varnothing_{\text{cum, i}}\right) \times \frac{K_{\text{cum, i}} + K_{\text{cum, i+1}}}{2} \quad (9)$$

The area of the plot below the line of perfect equality in Fig. 7 is equal to half the total area of the plot (a square), and so the area between the Lorenz curve and the line of perfect equality is equal to the total area below the Lorenz curve minus the area of the plot below the line of perfect equality.

In this study, the values of Lc, $\varnothing$, and K were calculated for each paleovalley of the Sarah Formation and arranged in descending order. Then, the cumulative sums were calculated and normalized to 1 Tables 8, 9, 10, 11, 12, 13, 14, 15, 16, 17, and 18), after which the normalized porosity values ($\sum\varnothing$) were plotted as a function of the normalized cumulative permeability values ($\sum$K) (Fig. 8).

The Lc values for the Bukayriyah, Hanadir, Sarah, and Khanasir Sarah paleovalleys are 0.30, 0.59, 0.58, and 0.54, respectively, indicating high variability in the distribution of porosity and permeability.

Summary of the heterogeneity parameters

Table 3 provides a comparison of the heterogeneity parameters for the Sarah Formation paleovalleys. The coefficient of variation values for permeability distributions is in the 0.63–1.93 range, indicating extremely heterogeneous distributions. The Dykstra-Parsons coefficient values are in the 0.56–0.88 range, suggesting very heterogeneous to extremely heterogeneous reservoirs (Tables 4, 5, 6, and 7). The Lorenz coefficients correlate well with the Dykstra-Parsons coefficients (Fig. 9 and Tables 8, 9, 10, 11, 12, 13, 14, 15, 16, 17, and 18).

Overall, the parameters indicate that the Sarah Formation paleovalleys represent heterogeneous to very heterogeneous reservoirs, and variations in porosity and permeability can be attributed to textural variation, compaction, cementation, dissolution, replacement, quartz overgrowth, and pore size distribution (El-Deek et al. 2014b).

Interpretation and discussion

Analysis of rocks exposed in paleovalleys of the Sarah Formation reveals approximately six lithofacies. The lithologies range from sandstone to siltstone to diamictite, some with a pebbly component. Horizontally laminated sandstone is the most common lithofacies, occupying approximately 60% of the total composite section. Petrographic analysis indicates that the sandstones are predominantly fine- to medium-grained, moderately to well-sorted quartz arenites. Alkali feldspars and plagioclase are the main detrital components of the samples. The grains are mainly sub-angular to sub-rounded. Mud is the predominant matrix type, but constitutes < 2% of the total rock volume. The cementing materials (5–10%) include clay and iron oxides, while SEM and XRD analyses show kaolinite to be the predominant cementing material. The abundance of kaolinite and ferruginous cement is responsible for the critical reduction in permeability, while the coating of quartz grains by kaolinite retards compaction, inhibits quartz overgrowth, and hence plays a significant role in preserving the initial porosity and permeability. Such preservation of porosity allows the dissolution of feldspar grains by pore fluids (e.g., meteoric water), which creates secondary porosity and subsequently enhances the permeability.

The heterogeneity of the Sarah Formation reflects the complexity of facies, paleoenvironments, and paleogeography of the Late Ordovician deposits, which makes the prediction of reservoir quality difficult, especially relying on insufficient borehole data. While the borehole data cannot resolve the relationship of such multiple closely spaced rock bodies, the outcrop analog of the Sarah Formation helps to investigate such complexity, as it provides information about rock body dimension, size, and orientation, thus revealing details on the reservoir continuity and connectivity within the glacio-fluvial environments and their vertical and lateral relationships with other Paleozoic formations at a resolution unavailable from the subsurface (Fig. 10). Such information is useful as it fills the gap in knowledge within the interwell spacing (Abdullatif and Makkawi 2010; Al-Ajmi et al. 2011; Grammer et al. 2004; North and Prosser 1993; Thurmond et al. 2005; Tye 2004).

Based on field observations and laboratory analyses, the heterogeneity of the Sarah Formation paleovalleys occurs at different scales. At the megascopic and macroscopic scales, the Late Ordovician glaciation resulted in the formation of unconformities and overlying glacial, glacio-marine, and glacio-fluvial deposits laid down as influxes into deeply incised paleovalleys cutting through various depositional environments, e.g., the storm-dominated, shallow marine depositional system of Hanadir and Kahfah, and the upper progradational sequence of the offshore marine Ra'an shale and the tide-dominated Quwarah sandstone. In addition, the Sarah Formation cuts further into the fluvial and shallow marine sandstones of the Saq Formation in Khanasir Sarah paleovalley (Clark-Lowes 2005). This indicates the basin-scale heterogeneity in terms of depositional environments that may be detected in a single borehole. At the mesoscopic scale, the depositional environments have impacted the lithofacies variability within the glacio-fluvial paleovalleys where several lithofacies were identified (e.g., Figs. 2, 3, and 4, Table 2). At the microscopic scale, these lithofacies vary in terms of texture (grain size, shape, roundness), composition of detrital mineralogy, and all superimposed diagenetic changes. This might eventually reflect on porosity and permeability variation within the paleovalleys.

Therefore, all these aspects discussed earlier collectively might be responsible for the heterogeneities as revealed from the statistical parameters (Table 3). Understanding the different scales of heterogeneity that occur in the Sarah Formation, from pore-scale to basin-scale, might help in better evaluating and predicting the reservoir quality and architecture in the subsurface.

Conclusions

The heterogeneity of the Sarah Formation reservoirs may be attributed to complex depositional and diagenetic variations that have affected the porosity and permeability distributions. Understanding the geologic controls on the variation of reservoir quality increases the understanding of reservoir heterogeneity in the subsurface and is a key factor for predicting the distribution of the potential reservoir facies, and their petrophysical properties.

The reservoir heterogeneity analysis conducted using the three statistical measures, coefficient of variation, Dykstra-Parsons coefficient, and Lorenz coefficient, shows that the Sarah Formation represents a heterogeneous to very heterogeneous reservoir. The integration of outcrop analog data with subsurface information may provide a better understanding of the glacio-fluvial reservoir quality and architecture.

Acknowledgments We would like to thank the Geosciences Department at King Fahd University of Petroleum and Minerals (KFUPM) for their support and assistance. Finally, we thank Dr. Khalid Al-Ramadan, Geosciences Department at KFUPM, for his comments on this work.

Funding Source We also acknowledge the funding support and help provided by the Deanship of Scientific Research for Project RCRG 1114 under the "Reservoir Characterization Research Group" at the Geosciences Department, KFUPM.

Appendix 1 Calculations of the Dykstra-Parsons coefficient

Table 4 Frequency distribution for the permeability measurements in Bukayriyah paleovalley

Sample no.	Probability	*K* (mD)*	Sample no.	Probability	*K* (mD)
S2H3	0.00	27.10	S2H8	0.50	10.29
S2H1	0.02	23.02	S1H1	0.52	9.98
S2H7	0.05	18.26	S2V4	0.55	9.19
S2V3	0.07	17.46	S1H6	0.57	9.03
S2V2	0.09	16.88	S1H4	0.59	8.56
S2V6 (c)	0.11	15.75	S1V2	0.61	8.28
S2H5	0.14	15.21	S1H2	0.64	8.21
S2H4	0.16	14.93	S1V12	0.66	4.68
S2H11	0.18	13.88	S1V13	0.68	4.37
S2H10	0.20	13.53	S1H13	0.70	3.82
S2V10	0.23	13.31	S1H8	0.73	3.44
S1V5	0.25	13.27	S1V11	0.75	3.38
S1V4	0.27	12.65	S1H9	0.77	3.33
S2H9	0.30	12.41	S1H7	0.80	3.27
S2V11	0.32	11.97	S1H12	0.82	3.22
S2V9	0.34	11.93	S1H11	0.84	2.52
S1V6	0.36	11.84	S1V9	0.86	2.38
S2V6 (a)	0.39	11.82	S1V7	0.89	1.91
S1H3	0.41	11.12	S1H10	0.91	1.89
S2V6 (b)	0.43	11.10	S1V8	0.93	1.87
S2V5	0.45	10.65	S1V10	0.95	1.81
S1H5	0.48	10.54	S1V3	0.98	1.00

* millidarcy

Table 5 Frequency distribution for the permeability measurements in Hanadir paleovalley

Layer no.	Probability	*K* (mD)	Layer no.	Probability	*K* (mD)
SR-2-V3	0	2252	SR-7A-H4	0.5	232.07
SR-2-H4	0.01	2160.1	SR-7A-V3	0.51	229.69
SR-2-H5	0.02	2040.8	SR-3-V5	0.52	40.178
SR-2-H1	0.03	2004.2	RC-1-H3	0.53	29.905
SR-2-H2	0.04	1857.6	RC-1-H1	0.54	28.018
SR-3-V2-C	0.05	1585.1	RC-1-H2	0.55	27.677
SR-7C-H3	0.06	1576.6	RC-1-H6	0.56	26.805
SR-4-V2	0.07	1503.7	SR-7B-H1	0.57	24.733
SR-4-V1	0.08	1485.3	RC-4-H4	0.58	23.498
SR-4-V3	0.09	1240.2	RC-1-H8	0.59	22.28
SR-7B-H2	0.1	1193.2	RC-1-V4	0.6	21.719
SR-2-H3	0.11	1147.2	RC-1-V3	0.61	20.763
SR-9-V3	0.12	1111.5	RC-1-V5	0.62	20.622
SR-4-H1	0.13	1055.1	RC-1-V6	0.63	20.521
SR-3-V4	0.14	1003	RC-1-V8	0.64	19.562
SR-9-V1	0.15	1000.5	RC-1-V7	0.65	18.867
SR-2-V2	0.16	996.48	RC-1-V2	0.66	17.761
SR-4-H2	0.17	963.76	RC-4-H1	0.67	16.755
SR-3-V2-A	0.18	939.52	RC-4-H2	0.68	16.249
SR-3-V2-B	0.19	897.46	RC-4-H3	0.69	15.399
SR-3-H3	0.2	870.87	RC-1-V1	0.7	14.893
SR-3-H1	0.21	839.26	RC-2-H3	0.71	14.6
SR-3-V1	0.22	832.58	RC-2-V2	0.72	14.489
SR-3-H2	0.23	814.86	RC-4-V4	0.73	13.385
SR-4-H3	0.24	810.52	RC-2-H1	0.74	13.044
SR-5-H4	0.25	787.22	RC-2-H2	0.75	11.719
SR-7C-H2	0.26	780.64	RC-2-V1	0.76	11.442
SR-9-V2	0.27	736.7	RC-2-H4	0.77	10.821
SR-7C-V3	0.28	736.01	RC-4-V1	0.78	10.354
SR-7C-V2	0.29	689.37	RC-5-H2	0.79	10.099
SR-7C-V1	0.3	635.54	RC-3-H1	0.8	9.4909
SR-1-V1	0.31	597.56	RC-5-H6	0.81	8.3195
SR-1-V2	0.32	592.18	RC-3-H2	0.82	7.7348
SR-5-V4	0.33	584.46	RC-3-V1	0.83	7.6898
SR-5-H3	0.34	584.15	RC-4-V3	0.84	7.5434
SR-1-H1	0.35	515.57	RC-4-V2	0.85	7.4648
SR-6-V1	0.36	504.9	RC-5-H1	0.86	7.3419
SR-5-H1	0.37	501.24	RC-5-H3	0.87	7.3026
SR-5-H2	0.38	458.22	RC-5-H5	0.88	6.9235
SR-5-V3	0.39	455.56	RC-4-V5	0.89	6.4892
SR-1-H2	0.4	437.2	RC-3-H3	0.9	6.0436
SR-6-H1	0.41	436.4	RC-5-V5	0.91	5.3379
SR-6-V2	0.42	401.25	RC-5-V2	0.92	5.1234
SR-7A-H2	0.43	399.23	RC-5-V1	0.93	4.9794
SR-6-H3	0.44	332.12	RC-5-V4	0.94	4.9101
SR-5-V1	0.45	328.71	RC-3-V2	0.95	4.3656
SR-5-V2	0.46	327.51	RC-3-V3	0.96	4.1178
SR-7A-H3	0.47	326.83	RC-3-H4	0.97	3.8329
SR-6-H2	0.48	297.63	RC-5-V3	0.98	2.8056
SR-7A-H1	0.49	243.33	RC-3-V4	0.99	2.7902

Table 6 Frequency distribution for the permeability measurements in Sarah paleovalley

Layer no.	Probability	*K* (mD)	Layer no.	Probability	*K* (mD)
SQ-1B-V1	0	757.48	SQ-4-H1	0.49	26.99
SQ-1B-V5	0.01	755.6	SQ-7-V3	0.51	26.57
SQ-1B-V6	0.02	750.41	SQ-6-H4	0.52	26.15
SQ-1B-V2	0.03	723.88	SQ-4-H2	0.53	26.04

Table 6 (continued)

Layer no.	Probability	*K* (mD)	Layer no.	Probability	*K* (mD)
SQ-1B-H1	0.04	721.37	SQ-7-H4	0.54	25.82
SQ-1B-V4	0.05	717.09	SQ-7-V4	0.55	25.37
SQ-1B-V3	0.06	713.88	SQ-5B-V3	0.56	25.28
SQ-1B-H2	0.07	675.06	SQ-6-H5	0.57	25.19
SQ-1A-H1	0.08	559.27	SQ-5A-H2	0.58	24.56
SQ-1A-V6	0.09	493.63	SQ-1A-V3	0.59	22.94
SQ-1A-H2	0.1	443.12	SQ-7-H2	0.6	22.78
SQ-1A-H3	0.11	432.28	SQ-7-H1	0.61	22.68
SQ-1C-V4	0.12	99.22	SQ-6-H2	0.62	22.67
SQ-1C-V2	0.13	94.81	SQ-4-V3	0.63	22.46
SQ-1C-V3	0.14	91.93	SQ-7-H3	0.64	21.59
SQ-1C-V1	0.15	90.11	SQ-5B-H7	0.65	20.92
SQ-1C-V7	0.16	90.01	SQ-5A-H4	0.66	20.32
SQ-1C-V5	0.18	84.6	SQ-5B-H8	0.67	20.27
SQ-1C-V6	0.19	75.92	SQ-4-V2	0.68	18.86
SQ-2A-H2	0.2	62.79	SQ-5B-H2	0.69	18.59
SQ-1C-H1	0.21	62.22	SQ-5A-H3	0.7	18.47
SQ-1C-H4	0.22	60.46	SQ-4-V1	0.71	18.35
SQ-1C-H3	0.23	56.64	SQ-5A-H1	0.72	18.09
SQ-2A-V3	0.24	52.61	SQ-5B-V5	0.73	17.87
SQ-1C-H2	0.25	52.58	SQ-5B-V2	0.74	16.1
SQ-2C-V1	0.26	52.33	SQ-5B-H5	0.75	14.48
SQ-2A-V4	0.27	49.33	SQ-6-H1	0.76	14.4
SQ-2C-V2	0.28	49.27	S3H6	0.77	11.63
SQ-2C-V3	0.29	49.2	SQ-5B-H6	0.78	11.53
SQ-2A-V2	0.3	48.84	S3H4	0.79	11.41
SQ-2A-V1	0.31	45.6	S3H8	0.8	11.17
SQ-2B-H2	0.32	44.31	S3H7	0.81	11.05
SQ-3-V3	0.33	37.84	S3V8	0.82	11.03
SQ-5B-H4	0.34	37.5	S3H5	0.84	11.01
SQ-3-V4	0.35	37.36	S3H2	0.85	10.89
SQ-3-H4	0.36	36.77	S3V5	0.86	10.74
SQ-3-H1	0.37	35.98	S3V6	0.87	9.98
SQ-3-V2	0.38	33.93	S3H1	0.88	9.89
SQ-5B-V1	0.39	32.75	S3V4	0.89	9.62
SQ-7-V2	0.4	32.42	S3V10	0.9	9.52
SQ-5B-H3	0.41	32.04	S3V1	0.91	9.45
SQ-5B-H1	0.42	31.88	S3V7	0.92	9.24
SQ-7-V1	0.43	31.45	S3V11	0.93	9.08
SQ-1A-V1	0.44	30.68	S3V9	0.94	8.63
SQ-5B-V4	0.45	29.79	S3V13	0.95	8.6
SQ-6-H6	0.46	29.21	S3V3	0.96	8.33
SQ-1A-V2	0.47	28.91	SQ-1A-V4	0.97	5.07
SQ-4-H3	0.48	27.61	SQ-3-V1	0.98	2.3
			SQ-1A-V5	0.99	1.26

Table 7 Frequency distribution for the permeability measurements in Khanasir Sarah paleovalley

Layer no.	Probability	*K* (mD)
KS-3C-H4	0.00	1628.70
KS-3C-V3	0.05	1056.50
KS-3C-H3	0.10	1047.10
KS-3C-H1	0.14	910.64
KS-3C-H2	0.19	910.42
KS-3C-V2	0.24	825.51
KS-3C-V1	0.29	706.26
KS-9-H3	0.33	206.60
KS-9-H6	0.38	191.46
KS-9-H4	0.43	180.36
KS-9-H5	0.48	172.76
KS-9-V3	0.52	89.73
KS-9-V4	0.57	88.68
KS-9-H2	0.62	70.50
KS-9-H1	0.67	60.61
KS-1-V1	0.71	46.62
KS-9-V1	0.76	46.29
KS-1-V4	0.81	42.39
KS-2-V2	0.86	39.53
KS-1-V3	0.90	39.42
KS-9-V2	0.95	7.41

Appendix 2 Calculations of the Lorenz Coefficient

Table 8 Calculation of Lorenz coefficient for porosity and permeability measurements from Bukayriyah paleovalley

φ	Cumulative	% cumulative	*K*	Cumulative	% cumulative
34.27	0.00	0.00	27.10	0.00	0.00
29.87	34.27	0.03	23.02	27.10	0.06
29.73	64.14	0.05	18.26	50.11	0.12
29.66	93.87	0.08	17.46	68.37	0.16
29.58	123.53	0.10	16.88	85.84	0.20
29.16	153.11	0.13	15.75	102.71	0.24
28.47	182.28	0.15	15.21	118.47	0.28
28.13	210.75	0.18	14.93	133.68	0.31
28.08	238.88	0.20	13.88	148.60	0.35
27.82	266.96	0.23	13.53	162.49	0.38
27.69	294.78	0.25	13.31	176.02	0.41
27.67	322.47	0.27	13.27	189.33	0.45
27.58	350.14	0.30	12.65	202.60	0.48
27.22	377.72	0.32	12.41	215.25	0.51
27.22	404.94	0.34	11.97	227.66	0.54
27.10	432.16	0.37	11.93	239.63	0.56

Table 8 (continued)

φ	Cumulative	% cumulative	K	Cumulative	% cumulative
27.06	459.26	0.39	11.84	251.56	0.59
26.99	486.32	0.41	11.82	263.40	0.62
26.95	513.31	0.44	11.12	275.22	0.65
26.93	540.26	0.46	11.10	286.34	0.67
26.79	567.18	0.48	10.65	297.43	0.70

Table 9 Calculation of Lorenz coefficient for porosity and permeability measurements from Bukayriyah paleovalley (continued)

φ	Cumulative	% cumulative	K	Cumulative	% cumulative
26.70	1.00	0.00	10.54	0.00	0.00
26.67	27.70	0.02	10.29	10.54	0.02
26.62	54.37	0.05	9.98	20.83	0.05
26.60	80.99	0.07	9.19	30.80	0.07
26.50	107.59	0.09	9.03	39.99	0.09
26.35	134.09	0.11	8.56	49.03	0.12
26.31	160.44	0.14	8.28	57.59	0.14
26.29	186.75	0.16	8.21	65.87	0.15
26.03	213.04	0.18	4.68	74.08	0.17
25.90	239.07	0.20	4.37	78.76	0.19
25.89	264.98	0.22	3.82	83.13	0.20
25.89	290.87	0.25	3.44	86.95	0.20
25.79	316.76	0.27	3.38	90.39	0.21
25.69	342.54	0.29	3.33	93.76	0.22
25.66	368.24	0.31	3.27	97.09	0.23
25.61	393.90	0.33	3.22	100.37	0.24
25.41	419.50	0.36	2.52	103.59	0.24
25.26	444.92	0.38	2.38	106.11	0.25
24.87	470.17	0.40	1.91	108.49	0.26
24.72	495.05	0.42	1.89	110.40	0.26
24.70	519.77	0.44	1.87	112.29	0.26
24.58	544.47	0.46	1.81	114.15	0.27
17.56	569.05	0.48	1.00	115.97	0.27
	586.62	0.50		116.97	0.28

Table 10 Calculation of Lorenz coefficient for porosity and permeability measurements from Hanadir paleovalley

φ	Cumulative	% cumulative	K	Cumulative	% cumulative
35.13	0.00	0.00	2252.00	0.00	0.00
34.62	36.13	0.01	2160.10	2252.00	0.05
32.84	70.75	0.03	2040.80	4412.10	0.10
32.70	103.58	0.04	2004.20	6452.90	0.14
31.74	136.28	0.05	1857.60	8457.10	0.18
31.67	168.02	0.06	1585.10	10,314.70	0.22
31.67	199.69	0.07	1576.60	11,899.80	0.26

Table 10 (continued)

φ	Cumulative	% cumulative	K	Cumulative	% cumulative
31.52	231.36	0.08	1503.70	13,476.40	0.29
31.37	262.88	0.09	1485.30	14,980.10	0.33
31.27	294.25	0.10	1240.20	16,465.40	0.36
30.98	325.53	0.12	1193.20	17,705.60	0.38
30.98	356.51	0.13	1147.20	18,898.80	0.41
30.83	387.48	0.14	1111.50	20,046.00	0.44
30.81	418.31	0.15	1055.10	21,157.50	0.46
30.81	449.13	0.16	1003.00	22,212.60	0.48
30.78	479.93	0.17	1000.50	23,215.60	0.50
30.74	510.71	0.18	996.48	24,216.10	0.53
30.65	541.46	0.19	963.76	25,212.58	0.55
30.62	572.10	0.20	939.52	26,176.34	0.57
30.56	602.72	0.21	897.46	27,115.86	0.59
30.45	633.28	0.23	870.87	28,013.32	0.61
30.41	663.73	0.24	839.26	28,884.19	0.63
30.32	694.14	0.25	832.58	29,723.45	0.65
30.31	724.46	0.26	814.86	30,556.03	0.66

Table 11 Calculation of Lorenz coefficient for porosity and permeability measurements from Hanadir paleovalley (continued)

φ	Cumulative	% cumulative	K	Cumulative	% cumulative
30.31	754.77	0.27	810.52	31,370.89	0.68
30.29	785.07	0.28	787.22	32,181.41	0.70
30.23	815.36	0.29	780.64	32,968.63	0.72
30.21	845.59	0.30	736.70	33,749.27	0.73
30.20	875.80	0.31	736.01	34,485.97	0.75
30.18	906.00	0.32	689.37	35,221.98	0.77
30.12	936.18	0.33	635.54	35,911.35	0.78
30.02	966.30	0.34	597.56	36,546.89	0.79
29.93	996.32	0.36	592.18	37,144.45	0.81
29.89	1026.25	0.37	584.46	37,736.63	0.82
29.86	1056.14	0.38	584.15	38,321.09	0.83
29.82	1086.00	0.39	515.57	38,905.24	0.85
29.77	1115.82	0.40	504.90	39,420.81	0.86
29.74	1145.59	0.41	501.24	39,925.71	0.87
29.70	1175.33	0.42	458.22	40,426.95	0.88
29.68	1205.04	0.43	455.56	40,885.17	0.89
29.67	1234.71	0.44	437.20	41,340.73	0.90
29.66	1264.38	0.45	436.40	41,777.93	0.91
29.54	1294.04	0.46	401.25	42,214.33	0.92
29.47	1323.58	0.47	399.23	42,615.58	0.93
29.37	1353.06	0.48	332.12	43,014.81	0.94
29.29	1382.42	0.49	328.71	43,346.93	0.94
29.20	1411.72	0.50	327.51	43,675.64	0.95
29.17	1440.92	0.51	326.83	44,003.15	0.96
29.13	1470.09	0.52	297.63	44,329.98	0.96

Table 12 Calculation of Lorenz coefficient for porosity and permeability measurements from Hanadir paleovalley (Contd.)

φ	Cumulative	% cumulative	K	Cumulative	% cumulative
29.02	1499.23	0.53	243.33	44,627.61	0.97
29.00	1528.25	0.54	232.07	44,870.94	0.98
28.72	1557.25	0.56	229.69	45,103.01	0.98
28.61	1585.97	0.57	40.18	45,332.70	0.99
28.60	1614.59	0.58	29.91	45,372.88	0.99
28.58	1643.18	0.59	28.02	45,402.78	0.99
28.54	1671.76	0.60	27.68	45,430.80	0.99
28.42	1700.30	0.61	26.81	45,458.48	0.99
28.40	1728.72	0.62	24.73	45,485.28	0.99
28.24	1757.11	0.63	23.50	45,510.02	0.99
28.22	1785.35	0.64	22.28	45,533.51	0.99
28.20	1813.57	0.65	21.72	45,555.79	0.99
28.15	1841.77	0.66	20.76	45,577.51	0.99
28.11	1869.92	0.67	20.62	45,598.28	0.99
28.09	1898.02	0.68	20.52	45,618.90	0.99
28.05	1926.11	0.69	19.56	45,639.42	0.99
27.97	1954.16	0.70	18.87	45,658.98	0.99
27.79	1982.13	0.71	17.76	45,677.85	0.99
27.76	2009.92	0.72	16.76	45,695.61	0.99
27.62	2037.69	0.73	16.25	45,712.36	0.99
27.61	2065.31	0.74	15.40	45,728.61	0.99
27.58	2092.91	0.75	14.89	45,744.01	0.99
27.02	2120.50	0.76	14.60	45,758.91	0.99
27.00	2147.52	0.77	14.49	45,773.51	1.00
27.23	2174.52	0.78	32.75	45,787.99	1.00

Table 13 Calculation of Lorenz coefficient for porosity and permeability measurements from Hanadir paleovalley (Contd.)

φ	Cumulative	% cumulative	K	Cumulative	% cumulative
26.79	2201.75	0.78	13.04	45,820.74	1.00
26.55	2228.54	0.79	11.72	45,833.78	1.00
26.45	2255.09	0.80	11.44	45,845.50	1.00
26.02	2281.53	0.81	10.82	45,856.94	1.00
25.98	2307.55	0.82	10.35	45,867.77	1.00
25.31	2333.53	0.83	10.10	45,878.12	1.00
25.31	2358.84	0.84	9.49	45,888.22	1.00
24.84	2384.15	0.85	8.32	45,897.71	1.00
24.77	2408.98	0.86	7.73	45,906.03	1.00
24.76	2433.76	0.87	7.69	45,913.76	1.00
24.21	2458.51	0.88	7.54	45,921.45	1.00
24.10	2482.72	0.88	7.46	45,929.00	1.00
24.09	2506.83	0.89	7.34	45,936.46	1.00

Table 13 (continued)

φ	Cumulative	% cumulative	K	Cumulative	% cumulative
23.62	2530.91	0.90	7.30	45,943.80	1.00
22.91	2554.53	0.91	6.92	45,951.11	1.00
22.58	2577.44	0.92	6.49	45,958.03	1.00
22.37	2600.02	0.93	6.04	45,964.52	1.00
22.06	2622.40	0.93	5.34	45,970.56	1.00
21.53	2644.46	0.94	5.12	45,975.90	1.00
21.37	2665.99	0.95	4.98	45,981.02	1.00
21.12	2687.36	0.96	4.91	45,986.00	1.00
21.06	2708.49	0.97	4.37	45,990.91	1.00
19.93	2729.55	0.97	4.12	45,995.28	1.00
19.37	2749.48	0.98	3.83	45,999.40	1.00
19.10	2768.85	0.99	2.81	46,003.23	1.00
19.05	2787.95	0.99	2.79	46,006.03	1.00
	2807.00	1.00		46,008.83	1.00

Table 14 Calculation of Lorenz coefficient for porosity and permeability measurements from Sarah paleovalley

φ	Cumulative	% cumulative	K	Cumulative	% cumulative
56.71	0.00	0.00	757.48	0.00	0.00
55.74	57.71	0.02	755.60	757.48	0.07
55.70	113.45	0.04	750.41	1513.08	0.15
55.22	169.15	0.06	723.88	2263.49	0.22
55.09	224.37	0.08	721.37	2987.37	0.29
54.47	279.46	0.10	717.09	3708.74	0.36
53.68	333.93	0.12	713.88	4425.83	0.43
53.42	387.61	0.14	675.06	5139.71	0.50
53.13	441.02	0.16	559.27	5814.77	0.56
52.86	494.16	0.18	493.63	6374.04	0.61
52.39	547.02	0.20	443.12	6867.67	0.66
51.13	599.41	0.22	432.28	7310.79	0.71
38.32	650.54	0.24	99.22	7743.07	0.75
37.47	688.85	0.26	94.81	7842.29	0.76
36.88	726.32	0.27	91.93	7937.10	0.77
35.08	763.21	0.28	90.11	8029.04	0.77
33.22	798.29	0.30	90.01	8119.15	0.78
33.17	831.51	0.31	84.60	8209.16	0.79
33.10	864.68	0.32	75.92	8293.75	0.80
33.08	897.77	0.33	62.79	8369.67	0.81
32.90	930.85	0.35	62.22	8432.46	0.81
32.64	963.75	0.36	60.46	8494.68	0.82
30.45	996.39	0.37	56.64	8555.14	0.83

Table 15 Calculation of Lorenz coefficient for porosity and permeability measurements from Sarah paleovalley (continued)

φ	Cumulative	% cumulative	K	Cumulative	% cumulative
28.17	1026.84	0.38	52.61	8611.78	0.83
27.98	1055.01	0.39	52.58	8664.38	0.84
27.73	1082.98	0.40	52.33	8716.96	0.84
27.19	1110.71	0.41	49.33	8769.29	0.85
26.31	1137.90	0.42	49.27	8818.62	0.85
25.07	1164.21	0.43	49.20	8867.88	0.86
25.07	1189.28	0.44	48.84	8917.08	0.86
24.93	1214.34	0.45	45.60	8965.92	0.86
24.64	1239.27	0.46	44.31	9011.52	0.87
24.45	1263.91	0.47	37.84	9055.83	0.87
24.33	1288.36	0.48	37.50	9093.67	0.88
24.28	1312.68	0.49	37.36	9131.17	0.88
24.26	1336.96	0.50	36.77	9168.53	0.88
24.11	1361.22	0.51	35.98	9205.30	0.89
24.04	1385.33	0.51	33.93	9241.28	0.89
24.02	1409.37	0.52	32.75	9275.21	0.89
24.01	1433.39	0.53	32.42	9307.97	0.90
23.94	1457.40	0.54	32.04	9340.39	0.90
23.89	1481.34	0.55	31.88	9372.43	0.90
23.79	1505.23	0.56	31.45	9404.31	0.91
23.76	1529.02	0.57	30.68	9435.75	0.91
23.48	1552.78	0.58	29.79	9466.43	0.91
23.47	1576.27	0.59	29.21	9496.22	0.92
23.38	1599.74	0.59	28.91	9525.43	0.92
23.37	1623.12	0.60	27.61	9554.33	0.92

Table 16 Calculation of Lorenz coefficient for porosity and permeability measurements from Sarah paleovalley (continued)

φ	Cumulative	% cumulative	K	Cumulative	% cumulative
23.36	1646.49	0.61	26.99	9581.94	0.92
23.30	1669.85	0.62	26.57	9608.93	0.93
23.24	1693.15	0.63	26.15	9635.50	0.93
23.23	1716.38	0.64	26.04	9661.65	0.93
23.21	1739.62	0.65	25.82	9687.69	0.93
23.11	1762.83	0.65	25.37	9713.51	0.94
23.04	1785.93	0.66	25.28	9738.88	0.94
23.00	1808.98	0.67	25.19	9764.16	0.94
22.92	1831.98	0.68	24.56	9789.35	0.94
22.89	1854.90	0.69	22.94	9813.92	0.95
22.87	1877.79	0.70	22.78	9836.85	0.95
22.82	1900.66	0.71	22.68	9859.64	0.95
22.81	1923.48	0.71	22.67	9882.31	0.95
22.56	1946.29	0.72	22.46	9904.98	0.96

Table 16 (continued)

φ	Cumulative	% cumulative	K	Cumulative	% cumulative
22.41	1968.85	0.73	21.59	9927.45	0.96
22.17	1991.25	0.74	20.92	9949.04	0.96
22.15	2013.42	0.75	20.32	9969.96	0.96
22.03	2035.57	0.76	20.27	9990.28	0.96
21.97	2057.60	0.76	18.86	10,010.55	0.97
21.97	2079.57	0.77	18.59	10,029.41	0.97
21.90	2101.54	0.78	18.47	10,048.00	0.97
21.85	2123.44	0.79	18.35	10,066.47	0.97
21.82	2145.30	0.80	18.09	10,084.81	0.97
21.76	2167.12	0.80	17.87	10,102.91	0.97
21.67	2188.88	0.81	16.10	10,120.78	0.98

Table 17 Calculation of Lorenz coefficient for porosity and permeability measurements from Sarah paleovalley (continued)

φ	Cumulative	% cumulative	K	Cumulative	% cumulative
21.32	2210.55	0.82	14.48	10,136.88	0.98
21.31	2231.88	0.83	14.40	10,151.36	0.98
21.22	2253.19	0.84	11.63	10,165.76	0.98
21.10	2274.40	0.84	11.53	10,177.40	0.98
20.90	2295.50	0.85	11.41	10,188.93	0.98
20.88	2316.40	0.86	11.17	10,200.33	0.98
20.81	2337.28	0.87	11.05	10,211.50	0.98
20.70	2358.09	0.88	11.03	10,222.55	0.99
20.69	2378.79	0.88	11.01	10,233.59	0.99
20.65	2399.48	0.89	10.89	10,244.60	0.99
20.65	2420.13	0.90	10.74	10,255.49	0.99
20.23	2440.79	0.91	9.98	10,266.23	0.99
20.21	2461.02	0.91	9.89	10,276.21	0.99
20.10	2481.23	0.92	9.62	10,286.11	0.99
20.08	2501.32	0.93	9.52	10,295.73	0.99
19.82	2521.41	0.94	9.45	10,305.25	0.99
19.71	2541.22	0.94	9.24	10,314.70	0.99
19.66	2560.93	0.95	9.08	10,323.95	1.00
19.50	2580.59	0.96	8.63	10,333.02	1.00
19.37	2600.09	0.97	8.60	10,341.66	1.00
19.34	2619.46	0.97	8.33	10,350.25	1.00
19.31	2638.80	0.98	5.07	10,358.58	1.00
19.26	2658.11	0.99	2.30	10,363.65	1.00
16.92	2677.37	0.99	1.26	10,365.95	1.00
	2694.29	1.00		10,367.22	1.00

Table 18 Calculation of Lorenz coefficient for porosity and permeability measurements from Khanasir Sarah paleovalley

φ	Cumulative	% cumulative	K	Cumulative	% cumulative
32.24	0.00	0.00	1628.70	0.00	0.00
29.60	32.24	0.06	1056.50	1628.70	0.19
29.30	61.84	0.11	1047.10	2685.20	0.32
29.13	91.14	0.16	910.64	3732.30	0.45
29.06	120.27	0.22	910.42	4642.94	0.55
28.73	149.33	0.27	825.51	5553.36	0.66
28.45	178.06	0.32	706.26	6378.87	0.76
28.42	206.51	0.37	206.60	7085.13	0.85
28.37	234.93	0.42	191.46	7291.73	0.87
28.17	263.30	0.48	180.36	7483.19	0.89
27.87	291.47	0.53	172.76	7663.55	0.92
24.82	319.34	0.58	89.73	7836.31	0.94
24.79	344.16	0.62	88.68	7926.04	0.95
24.76	368.96	0.67	70.50	8014.72	0.96
24.04	393.71	0.71	60.61	8085.22	0.97
23.54	417.75	0.75	46.62	8145.83	0.97
23.36	441.29	0.80	46.29	8192.45	0.98
23.17	464.65	0.84	42.39	8238.73	0.98
23.12	487.82	0.88	39.53	8281.12	0.99
21.60	510.94	0.92	39.42	8320.65	0.99
20.95	532.54	0.96	7.41	8360.07	1.00
	553.49	1.00		8367.48	1.00

References

Abdulkadir IT, Sahin A, Abdullatif OM (2010) Distribution of petrophysical parameters in the Cambro-Ordovician Dibsiyah member of the Wajid sandstone, SW Saudi Arabia. J Pet Geol 33:269–280

Abdullatif OM (2011) Facies, depositional environment and sandstone composition of the Late Ordovician glacio-fluvio Sanamah Member, Wajid Formation, South West Saudi Arabia. Paper presented at the EGU General Assembly 2011, Vienna, Austria, 03–08 April 2011

Abdullatif O, El-Deek I, Abdulrazaq A, Osman M, Bashiri M (2013) Sedimentary facies and architecture of the outcropping Late Ordovician glacial paleovalley of north and south western Saudi Arabia. Paper presented at the 30th IAS Meeting of Sedimentology, University of Manchester, Manchester, United Kingdom, 2–5 September 2013

Abdullatif O, Makkawi M (2010) Virtual outcrop models: case study from the Paleozoic sandstone reservoir and aquifer analogs, Saudi Arabia. In: 72nd EAGE Conference and Exhibition-Workshops and Fieldtrips

Adams EW, Grélaud C, Pal M, Csoma AÉ, Al Ja'aidi OS, Al Hinai R (2011) Improving reservoir models of cretaceous carbonates with digital outcrop modeling (Jabal Madmar, Oman): static modeling and simulating clinoforms. Pet Geosci 17:309–332

Ahmed T (2010) Chapter 4–Fundamentals of Rock Properties. In: Reservoir Engineering Handbook. Gulf Professional Publishing, pp 189–287

Al-ajmi MF, El-Daoushy A, Ashkanani F, Saleh I, Pathak A, Hamadi H (2011) Innovative Pattern Balancing and Waterflood Optimization of a Super Giant Carbonate Mauddud Reservoir, Raudhatain Field, North Kuwait. In: SPE Digital Energy Conference and Exhibition. Society of Petroleum Engineers

Ali SA, Clark WJ, Moore WR, Dribus JR (2010) Diagenesis and reservoir quality. Oilfield Review 22:14–27

Al-Mahmoud MJ Al-Ghamdi I (2010) An Overview of Tight Gas Reservoirs in Saudi Arabia. In: Second EAGE Middle East Tight Gas Reservoirs Workshop

Al-Zayer A, Mesdour R, Al-Faleh K, Basri M, Utaibi A (2013) Practical Well Testing Analysis Considerations in Heterogeneous Sandstone. In: SPE Saudi Arabia Section Technical Symposium and Exhibition. Society of Petroleum Engineers

Boggs S (2006) Principles of sedimentology and stratigraphy, 4th edn. Pearson Prentice Hall, Upper Saddle River

Briner A, Hulver M, Azzouni A Harvey C (2010) Regional Reservoir Quality of a Tight Gas Play: the Ordovician Sarah Formation in the Rub'Al Khali Basin of Southern Saudi Arabia. In: Second EAGE Middle East Tight Gas Reservoirs Workshop

Clark-Lowes DD (2005) Arabian glacial deposits: recognition of palaeovalleys within the Upper Ordovician Sarah Formation, Al Qasim district, Saudi Arabia. Proc Geol Assoc 116:331–347

Dykstra H, Parsons R (1950) The prediction of oil recovery by waterflood. In: Secondary recovery of oil in the United States, vol 2. American Petroleum Institute. Division of Production, New York, pp 160–174

El-Deek I, Abdullatif O (2013) Characterization of reservoir quality from the outcrop analog for the Palaeozoic Sarah Formation glacial and fluvial reservoirs, Qaseem area, Saudi Arabia. Paper presented at the KFUPM Graduate Research Day 2013, King Fahd University of Petroleum & Minerals, Dhahran, Saudi Arabia, Feb 03–04, 2013

El-Deek I, Abdullatif O, Al-Ramadan K, Korvin G (2013) Reservoir heterogeneity and quality of the Late Ordovician Sarah Formation: outcrop analog for tight gas sandstone, Saudi Arabia. Paper presented at the 10th Meeting of the Saudi Society for Geosciences (Geosciences for Sustainable Development), King Fahd University of Petroleum & Minerals, Dhahran, Saudi Arabia, April 15–17, 2013

El-Deek I, Abdullatif O, Korvin G, Al-Ramadan K (2014a) Diagenesis and reservoir heterogeneity of the Sarah Formation tight gas sandstones in central Saudi Arabia: a petrographical approach. Paper presented at the 2014 LIPE & AAPG Northern Arabia Geoscience Conference and Exhibition, Beirut, Lebanon, 27–29 May 2014

El-Deek I, Abdullatif O, Korvin G Al-Ramadan K (2014b) Inetegration of Sedimentology, Petrophysics and Statistics for Characterizing the Reservoir Heterogeneity of the Late Ordovician Sarah Formation, Central Saudi Arabia. In: EGU General Assembly Conference Abstracts, Vienna, Austria

Evans D, Lathon R, Senalp M, Connally T (1991) Stratigraphy of the Wajid Sandstone of Southwestern Saudi Arabi. In: Middle East Oil Show. Society of Petroleum Engineers

Fitch P, Davies S, Lovell M, Pritchard T (2013) Reservoir quality and reservoir heterogeneity: petrophysical application of the Lorenz coefficient. Petrophysics 54:465–474

Fitch PJ, Lovell MA, Davies SJ, Pritchard T, Harvey PK (2015) An integrated and quantitative approach to petrophysical heterogeneity. Mar Pet Geol 63:82–96

Gier S (2000) Clay mineral and organic diagenesis of the Lower Oligocene Schöneck Fishshale, western Austrian Molasse Basin. Clay Miner 35:709–717

Grammer GM, Harris PM, Eberli GP (2004) Integration of outcrop and modern analogs in reservoir modeling: overview with examples from the Bahamas. AAPG Mem 80:1–22

Higley DK, Pantea MP, Slatt RM (1997) 3-D reservoir characterization of the House Creek oil field, Powder River basin, Wyoming. Data series no. 33, V1.00. edn. U.S. Geological Survey, Reston

Jennings J Jr, Ward W (2000) Geostatistical analysis of permeability data and modeling of fluid-flow effects in carbonate outcrops. SPE Reserv Eval Eng 3(04):292–303

Jensen JL (2000) Statistics for petroleum engineers and geoscientists, 2nd edn. Elsevier, Amesterdam

Kassab MA, Teama MA, Cheadle BA, El-Din ES, Mohamed IF, Mesbah MA (2015) Reservoir characterization of the Lower Abu Madi Formation using core analysis data: El-Wastani gas field, Egypt. J Afr Earth Sci 110:116–130

Ketzer JM, Morad S, Evans R, Al-Aasm I (2002) Distribution of diagenetic alterations in fluvial, deltaic, and shallow marine sandstones within a sequence stratigraphic framework: evidence from the Mullaghmore Formation (Carboniferous), NW Ireland. J Sediment Res 72:760–774

Khalil MH (2012) Reservoir Sweet Spots in the Arabian Petroleum Basin; Types and Controls. In: GEO, 2e012

Konert G, Afifi AM, Al-Hajri S, De Groot K, Al Naim A, Droste H (2001) AAPG Memoir 74, Chapter 24: Paleozoic stratigraphy and hydrocarbon habitat of the Arabian Plate 483–515

Lake L, Jensen J (1991) A review of heterogeneity measures used in reservoir characterization. In Situ 15(4):409–440

Lorenz MO (1905) Methods of measuring the concentration of wealth. Publ Am Stat Assoc 9:209–219

McClure H (1978) Early Paleozoic glaciation in Arabia. Palaeogeogr Palaeoclimatol Palaeoecol 25:315–326

McGillivray J, Husseini M (1992) The Paleozoic petroleum geology of central Arabia (1). AAPG Bull 76:1473–1490

Miall AD (1996) The geology of fluvial deposits: sedimentary facies, basin analysis, and petroleum geology. Springer, Berlin

Milliken KL (2001) Diagenetic heterogeneity in sandstone at the outcrop scale, Breathitt Formation (Pennsylvanian), eastern Kentucky. AAPG Bull 85:0795–0816

Morad S, Al-Ramadan K, Ketzer JM, De Ros L (2010) The impact of diagenesis on the heterogeneity of sandstone reservoirs: a review of the role of depositional facies and sequence stratigraphy. AAPG Bull 94:1267–1309

Morton-Thompson D, Woods AM (1993) Development geology reference manual: AAPG methods in exploration series, no. 10. American Association of Petroleum Geologists, Tulsa

Moscariello A, Spaak P, Jourdan A, Azzouni A-H (2009) The Ordovician glaciation in Saudi Arabia - exploration challenges Part 1: Geology (outcrop, subsurface, analogues). Search and Discovery Article #50175, adapted from oral presentation at AAPG International Conference and Exhibition, Cape Town, South Africa, October 26–29, 2008 http://www.searchanddiscovery.com/pdfz/documents/2009/50175moscariello/presentation.pdf.html

North CP, Prosser DJ (1993) Characterization of fluvial and aeolian reservoirs: problems and approaches. Geol Soc Lond Spec Publ 73:1–6. doi:10.1144/GSL.SP.1993.073.01.01

Peters EJ (2012) Advanced petrophysics: geology, porosity, absolute permeability, heterogeneity, and geostatistics, vol 1. Live Oak Book Company, Austin

Pranter MJ, Reza ZA, Budd DA (2006) Reservoir-scale characterization and multiphase fluid-flow modeling of lateral petrophysical heterogeneity within dolomite facies of the Madison Formation, Sheep Canyon and Lysite Mountain, Wyoming, USA. Pet Geosci 12:29–40

Razzaq W, Abdullatif O, Sahin A Hariri M (2014) Sedimentological and Petrophysical Heterogeneity of Glaciogenic Paleovalley, Late Ordovician Sarah Formation, Central Saudi Arabia. In: EGU General Assembly Conference Abstracts, Vienna, Austria

Sahin A, Saner S (2001) Statistical distributions and correlations of petrophysical parameters in the Arab-D reservoir, Abqaiq oilfield, eastern Saudi Arabia. J Pet Geol 24:101–114

Sahoo H, Gani MR, Hampson GJ, Gani ND, Ranson A (2016) Facies-to sandbody-scale heterogeneity in a tight-gas fluvial reservoir analog: Blackhawk Formation, Wasatch Plateau, Utah, USA. Mar Pet Geol. doi:10.1016/j.marpetgeo.2016.02.005

Schmalz J, Rahme H (1950) The variation of waterflood performance with variation in permeability profile. Producers Mon 15:9–12

Selley RC (1998) Elements of petroleum geology. Academic Press, San Diego

Senalp M, Al-Laboun A (2000) New evidence on the Late Ordovician glaciation in central Saudi Arabia. Saudi Aramco J Technol 11–40

Sun S, Shu L, Zeng Y, Cao J, Feng Z (2007) Porosity–permeability and textural heterogeneity of reservoir sandstones from the Lower Cretaceous Putaohua member of Yaojia Formation, Weixing oilfield, Songliao Basin, Northeast China. Mar Pet Geol 24:109–127

Surdam RC, Crossey LJ, Hagen ES, Heasler HP (1989) Organic-inorganic interactions and sandstone diagenesis. AAPG Bull 73:1–23

Thurmond JB, Drzewiecki PA, Xu X (2005) Building simple multiscale visualizations of outcrop geology using virtual reality modeling language (VRML). Comput Geosci 31(7):913–919

Tiab D, Donaldson EC (2004) Petrophysics: theory and practice of measuring reservoir rock and fluid transport properties, 2nd edn. Elsevier, New York

Tye RS (2004) Geomorphology: an approach to determining subsurface reservoir dimensions. AAPG Bull 88(8):1123–1147

Vaslet D (1987) Early Paleozoic glacial deposits in Saudi Arabia, a lithostratigraphic revision: technical record BRGM-TR-07, vol 1. Deputy Ministry for Mineral Resources, Saudi Arabia

Vaslet D (1989) Late Ordovician glacial deposits in Saudi Arabia: a lithostratigraphic revision of the Early Paleozoic succession. Ministry of Petroleum and Mineral Resources Deputy Ministry for Mineral Resources, Saudi Arabia

Vaslet D (1990) Upper Ordovician glacial deposits in Saudi-Arabia. Episodes 13:147–161

Wilson MD (ed) (1994) Reservoir quality assessment and prediction in clastic rocks. SEPM Publications, U.S.